Nanotechnology **20** (2009) 095205 (5pp) doi:10.1088/0957-4484/20/9/095205

The modification of Si nanocrystallites embedded in a dielectric matrix by high energy ion irradiation

I V Antonova[1], M B Gulyaev[1], A G Cherkov[1], V A Volodin[1], D V Marin[1], V A Skuratov[2], J Jedrzejewski[3] and I Balberg[3]

[1] Institute of Semiconductor Physics, Siberian Division of the Russian Academy of Sciences, Lavrentieva 13, Novosibirsk 630090, Russia
[2] Joint Institute for Nuclear Research, Dubna, 141980, Russia
[3] The Racah Institute of Physics, The Hebrew University, Jerusalem 91904, Israel

E-mail: antonova@isp.nsc.ru

Received 15 May 2008, in final form 24 November 2008
Published 6 February 2009
Online at stacks.iop.org/Nano/20/095205

Abstract
We have followed the effects of heavy ion irradiation on the structural, electrical, and photoluminescence properties of ensembles of silicon nanocrystallites embedded in a dielectric (SiO_2) matrix. This was done as a function of the irradiation dose and the content of the Si phase. The results obtained can be accounted for self-consistently assuming that a relatively small dose of the irradiation enhances the crystallization while for higher doses the irradiation enhances the amorphization. The corresponding processes suggest that tuning of the above properties can be achieved by swift heavy ion irradiation.

1. Introduction

Among a number of competing approaches towards nanoelectronics (for example, the use of self-organizing nanostructures, molecular electronics, nanomanipulations, and nanolithography), the idea of using non-overlapping swift heavy ion tracks is an attractive and a low-cost way to realize variants [1, 2]. The swift-heavy ion tracks created in dielectric or semiconductor materials have been demonstrated to provide new and unexpected properties, such as the occurrence of negative differential resistances [1] as well as the creation of conducting channels by etched ion tracks in silicon oxide and silicon oxynitride and filling-up of these nanometric pores with highly resistive or semiconductor matter for electronic and spintronic applications [2]. The subject of ion-beam-induced effects in silicon has recently regained much attention following the nanoscaling of Si structures [3]. In particular, crystallization versus amorphization due to the ion bombardment by various ions has been shown to significantly change the structural and optical properties of Si nanocrystallites that are embedded in insulating matrices [4–7]. While the previous studies have concentrated on these properties, in particular the photoluminescence (PL), the consequences of the ion irradiation on the corresponding electrical properties have not been reported. Following our recent understanding of the interplay between the above properties [8], we turn here to follow and evaluate the effects of swift heavy ion irradiation on systems of Si nanocrystallites (Si-ncs) embedded in SiO_2. We note that the special feature of this irradiation, in contrast with conventional implantation, is the large energy loss of the ions that takes place in the lattice of the target while creating a relatively low defect concentration in it [9–11]. This, as in the structures to be described below, is in particular the case, when the thickness of the studied layer is considerably smaller than the ion-projectile range. Hence, while in practice the defects are introduced in the substrate of the Si/SiO_2 films, the energy is mainly dissipated in the layer. For this study we applied the, so far unused, parameter of the density of the Si-ncs that enables not only the consideration of the effect of irradiation on the individual crystallites, as done in the previous works [4–7], but also the understanding of the, so far unstudied, electrical networks that are developed between them.

2. Experimental details

The samples used in the present study were fabricated as we have described in detail previously [8, 12] by the co-sputtering

of Si and quartz that yielded films with a variable Si content and thickness of ∼400 nm, on n-type Si wafer substrates with a resistivity of 1 Ω cm. The Si phase content in the sputtered films was determined from the thicknesses of the layers [13, 14] and is characterized by the volume percentage of the Si phase, x. Our films were deposited along a 100 mm long substrate, such that samples with x values between 5 and 94 vol% were obtained. After the film deposition all samples (SiO-1, SiO-2, and SiO-3) were annealed at 1150 °C for 50 min in order to form silicon nanocrystallites within the SiO_2 matrix [8]. For the purpose of this study we note that under these conditions the Si phase may consist of Si-ncs and amorphous silicon (a-Si) inclusions [8, 15]. One of these samples (hereafter the reference sample) is denoted below as SiO-1.

In our study we irradiated the samples with Bi, Kr, and Xe ions with different ion energies and different doses. Since the conspicuous qualitative features were much the same we describe here mainly the features of the Si-nc/SiO_2 samples that were subjected to irradiation by Bi ions with an energy of 670 MeV. This was done for the doses 1×10^{12} (sample SiO-2) and 8×10^{12} cm^{-2} (sample SiO-3). The commonly used analysis of such irradiation for crystalline Si or SiO_2 (SRIM code) targets suggests [9, 10] an ion-projectile penetration range of about 42 μm with a half width of the range which is around 0.75 μm. The electron stopping loss dE_e/dx in the layer is expected to vary between 24.3 keV nm^{-1} (for the SiO_2 end of the sample) and 22.0 keV nm^{-1} (for the Si end of the sample). The very small number of primary defects (vacancies) that are expected (from SRIM data [9–11]) to be introduced by one ion in our layers is in the range between 0.4 (for SiO_2) and 0.7 V/ion/nm (for Si). In practice all the ions, after their penetration, reside in the silicon substrate. The irradiated samples (SiO-2 and SiO-3) were subjected to additional annealing at 800 °C for 15 min in N_2 ambient in order to eliminate the electrically active radiation defects of deep levels in the Si wafer substrate [11], without changing the structure that was established in the Si-nc/SiO_2 layers by the 1150 °C annealing.

In the present study, our structural characterization tools were transmission electron microscopy (TEM) and Raman scattering spectroscopy. Since our applications of these methods have been detailed previously ([8] and [18], and [16] and [17], respectively) they will not be described here. However, it is important to note that the first technique provides information on the crystallite size and shape, while the Raman spectra provide a measure for the relative content of the Si crystallite phase (by its sharp 521 cm^{-1} peak) and the amorphous phase (by its broad 480 cm^{-1} peak) [17]. Peaks in the 520–510 cm^{-1} regime reveal the formation of small (<10 nm) crystallites [17].

For the electrical measurements, Ag contacts, with an area of 5×10^{-3} cm^{-2}, were deposited on the Si-nc/SiO_2 films, and an InGa alloy contact that served as a counter electrode was made to the substrate. Current–voltage (I–V) characteristics for the thus obtained vertical Ag[Si-nc/SiO_2]Si structures were then measured for the different x-values along these films.

The photoluminescence (PL) spectra were measured in the back-scattering configuration with excitation from an Ar-ion laser with a wavelength of 488 nm [12]. The corresponding measured signals were normalized by the spectral selectivity of the detector. All the measurements reported here were carried out at room temperature. In particular, for completeness let us mention that our previous detailed studies [18] of the PL (on samples prepared by the same procedure) have shown a shift of the PL peak with the variation of the size of the nanocrystallites in an apparent agreement with the expected quantum confinement. Moreover, we have provided a model for the mechanism that explains the manifestations of the quantum confinement in the observed PL. Below we will use these premises for the interpretation of the present results.

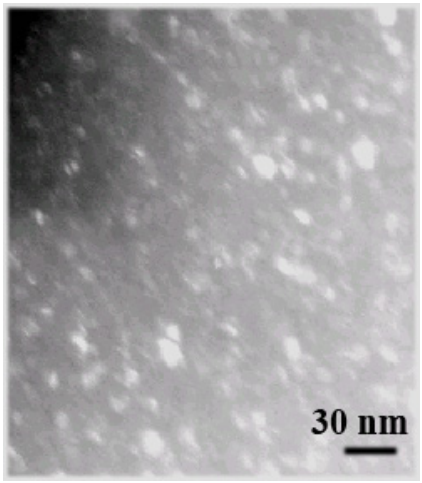

Figure 1. A cross section TEM image after irradiation with Xe and annealing treatment of the sample. The dose used was 10^{12} cm^{-2} and the silicon content was about 37 vol%. Note the 'linear' string of crystallites along the direction of the ion tracks.

3. Structural and optical properties of the modified Si nanocrystals

Starting with the structural data, we see in figure 1 a TEM image of sample SiO-2 after a relatively small-dose irradiation. Prior to irradiation the nanocrystallites, as we have shown previously [8, 18], have a spherical shape and a random distribution in the oxide. The important observation here, however, is the string of crystallites along the ion-projectile tracks. Comparison of the images from the non-irradiated samples [8, 18] with the present ones as given in figure 1 indicates the enhancement of crystallization along the tracks under the corresponding conditions of (relatively) weak irradiation.

Turning to the comparison of the Raman spectra of initial and the heavily irradiated samples (SiO-1 and SiO-3), in the Si-rich region (78% of Si content) where the Raman signal is appreciable we found that the crystalline Si Raman line at 521 cm^{-1} has decreased in its intensity by a factor 2.7 while the relative contribution of the amorphous line at 480 cm^{-1} has increased significantly. To demonstrate the first effect we have normalized the two spectra at the 521 cm^{-1} line. To demonstrate the second effect, we have subtracted the two original spectra. The result of this subtraction is shown in the

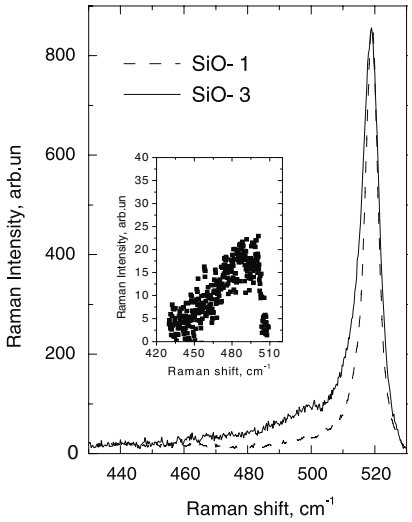

Figure 2. Raman spectra of a Si-nc/SiO_2 layer on a Si substrate for the initial sample SiO-1 and for the heavily irradiated sample SiO-3 at the sample location with a Si volume content of 78%. The curve for SiO-3 was multiplied by a factor 2.7 for normalization at the crystalline Si peak. In the inset we show the difference between the two original spectra in order to demonstrate the added intensity around the 'amorphous' 480 cm^{-1} line following the heavy irradiation.

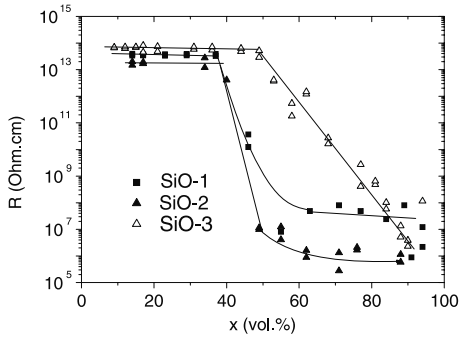

Figure 3. The resistivity (for an applied bias of 5 V) as a function of the Si phase content (vol%) for the reference (SiO-1) and weakly irradiated (SiO-2 and SiO-3) samples.

inset of figure 2. Noting that there is a significant contribution to the 521 cm^{-1} line from the substrate, the weakening of this line and the relative increase of the 480 cm^{-1} feature (beyond 510 cm^{-1} [19]) suggest that a significant amorphization of the film takes place upon heavy irradiation. We will demonstrate below that these conclusions are also confirmed indirectly by the conductivity and PL data.

We measured the I–V characteristics for different values of x on the reference sample as well as on the irradiated samples. This yielded the resistivity, R, of the Si-nc/SiO_2 layers as a function of x. In figure 3 we show the $R(x)$ dependence for an applied voltage of 5 V. For the reference sample SiO-1 a percolation transition with a threshold at about $x = 40$ vol% is found to yield a resistivity increase of about six orders of magnitude. For the sample SiO-2 (that was irradiated with a relatively small dose (1×10^{12} cm^{-2})) the percolation transition is seen to be slightly narrower, and the resistivity of the Si-nc/SiO_2 layer, above the percolation threshold, is about two orders of magnitude lower than that of the reference sample SiO-1. Irradiation with the higher ion dose (SiO-3) leads to a significant broadening of the percolation transition and to a higher resistivity for all x values.

The PL spectra for the reference and the irradiated samples for some x values are presented in figure 4. The PL peak of the reference sample SiO-1 that was found at ∼785 nm shows a slight shift with x here. After irradiation, the main spectral features of the spectra remain the same, but the irradiated samples exhibited a very strong increase (SiO-2) or a very strong decrease (SiO-3) of the PL intensity, and a much more pronounced shift of the spectral PL peak on the one hand, and its x-position shift to lower Si contents, on the other hand. The PL intensity as a function of the Si content $I_{PL}(x)$ is summarized in figure 4(d). These results suggest that there is a bimodal distribution of the crystallites size in our samples in accordance with our previous analysis of the green and red PL [15], such that the larger crystallites dominate the spectra of the reference sample and the weakly radiated sample, while the few smaller crystallites that remain after the irradiation dominate the spectra of the strongly irradiated sample.

4. Discussion

Before discussing our data, let us review very briefly the known effects of energetic ion bombardment on a semiconductor [3, 20] and the effects of annealing [14] on the properties that we study here. Considering previous estimates (known as the thermal spike model [9, 10]) and the fact that it causes an additional annealing due to the large electronic energy losses of the ions, one can estimate from SRIM data that the number of vacancies induced is less than 10^{14}–10^{15} cm^{-2} for the doses used (10^4–10^5 times smaller than the concentration of the nanocrystallites). Using the electron loss in our case of SiO_2, $dE_e/dx = 24.3$ keV nm^{-1}, and the dependence of the size of the ion tracks in α-SiO_2 [9, 10], we can further estimate the ion track to have a width of ∼5–6 nm such that the local transient temperature along the track can be as high as 2500 °C. This means that practically all the bonds between the atoms along the ion tracks can be broken and that the atoms are 'free' and able to have large displacements. This can bring about new bonds and a consequent amorphization due to the rapid quenching [3, 20, 21]. One more effect has to be taken into consideration for materials that are subjected to irradiation with high energy ions. This is the ion-beam-induced anisotropic plastic deformations [22, 23]. The anisotropy is related to the direction of the ion beam: materials expand perpendicular to the ion beam and contract parallel to it, while maintaining their volume. The anisotropic deformation increases with ion fluence and can change the shape of nanoparticles from spherical to ellipsoidal [22, 23].

On the other hand, we know (following our TEM and Raman scattering data) that the (as co-sputtered) films consist of a (non-hydrogenated) amorphous silicon (a-Si) network that is embedded in a SiO_2 matrix [8, 15]. Upon annealing at above 1000 °C, we found that, in our samples, crystallites were

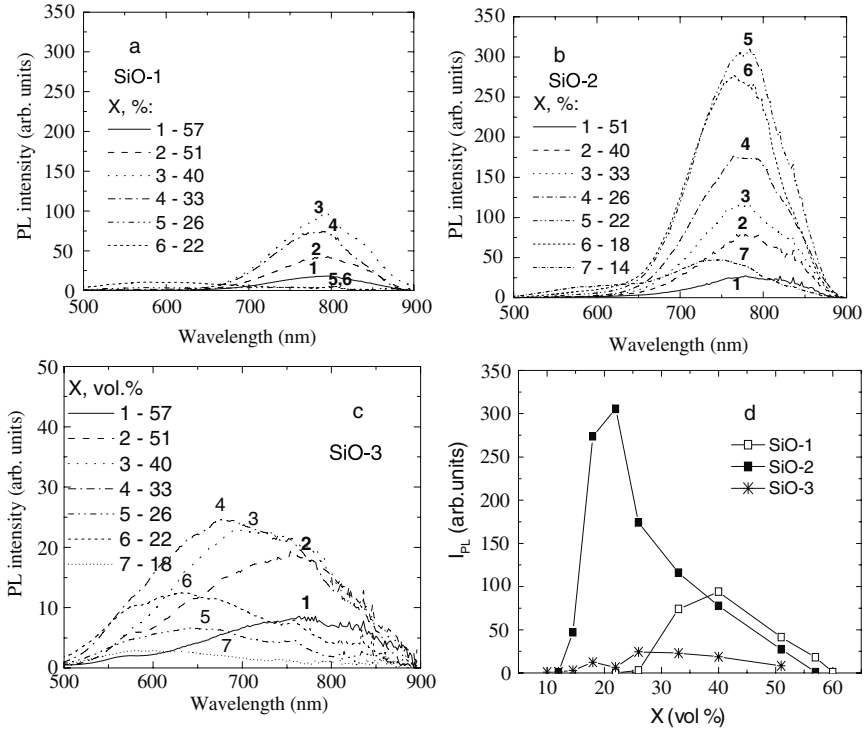

Figure 4. The PL spectra of specimens with different Si contents for some of our Si-nc/SiO_2 composites: SiO-1 (a), SiO-2 (b), and SiO-3 (c). These results are summarized (d) by the dependence of the PL intensity of the main peak on the Si content in our samples SiO-1 (785 nm), SiO-2 (785 nm), and SiO-3 (780–580 nm).

formed with sizes increasing from 2 nm (at the SiO_2 end) to about 10 nm (at the Si-rich end) [15, 18]. It is found that slight changes in the local annealing temperature in the range 1000–1150 °C affect the relative a-Si/Si-nc composition and thus the electrical and PL behaviors, explaining the great sensitivity of the structure to low-dose irradiation. Of course, the higher the annealing temperature the larger the Si-nc content and the larger the crystallite size. On the other hand, we found a strong green PL (at 560 nm) at the lower end of the above temperature interval and have shown that it is associated with crystallites the size of which corresponds to the smaller sizes that were mentioned above [15].

The above results can be interpreted self-consistently as follows. The width of the percolation transition is well known [24] to be narrower the higher the conductivity of the conductive filler. Expecting a higher conductivity for the crystalline phase than for the a-Si phase, the narrower percolation transition is induced with the creation of more crystallites (at the expense of the a-Si phase) as evidenced from our TEM images and as also found to be the case in implantation studies [5]. Thus, crystallization is found to prefer the part of sample with a relatively low Si content. For the other part of the sample, with the higher silicon content (about and above the percolation threshold), and for the higher doses, the amorphization of the Si nanocrystallites becomes preferred. The amorphization of the Si phase is a well-known effect for higher doses of ions with lower energies [20, 21]. The creation of more crystallites and the corresponding increase of the average conductivity of the 'filler', at large (above percolation) x values, also explain the lower resistivity in SiO-2 in comparison with the SiO-1 and SiO-3 samples. Our previous [8] association of the PL with individual, geometrically isolated, crystallites suggests here too that the enhancement of the PL is associated with the increase in the concentration of the crystallites, while the quenched PL (for the higher dose) is associated with their disappearance. The wide distribution of the PL spectra for the higher-dose irradiation (SiO-3) and its shift towards larger photon energies is consistent, in view of quantum confinement [18], with the existence of crystallites that are smaller than those prepared by our standard (SiO-1) annealing procedure [15]. These can be either residual crystallites that escaped the amorphization and/or crystallites that were newly generated during that process.

Following the above analysis of the structural changes and the physical properties, we suggest that, under the smaller dose that we used here, there is a local heating effect that induces crystallization just beyond our standard (and rather moderate) annealing process that is determined by its temperature, its duration, and the value of x (as was found to be the case in similar systems [18]). On the other hand, for the higher dose, considering the above-mentioned high temperatures and the possibility of overlapping ion tracks, the network melts on larger scales and the consequent rapid quenching yields its amorphization [20, 21].

5. Conclusions

We found that swift heavy ion irradiation can enhance or quench the formation of silicon nanocrystallites in an

embedding matrix according to the dose applied. We have correspondingly shown that both the electrical and the optical properties are improved under the smaller dose and are jeopardized under the larger dose. This suggests that a combination of proper annealing and ion irradiation could be used to optimize the properties of the above structures as requested.

Acknowledgments

This study was supported in part by the Russian Foundation of Basic Research (Project No. 06-02-72003, 08-02-00221) and in part by the Israel Science Foundation and the Israeli Ministry of Science and Technology. IB holds the Enrique Berman chair of Solar Energy Research at the HU.

References

[1] Fink D, Chadderton L T, Hoppe K, Fahrner W R, Chandra A and Kiv A 2007 *Nucl. Instrum. Methods* B **261** 727
[2] Fink D *et al* 2004 *Nucl. Instrum. Methods* B **218** 355
[3] For a comprehensive review see Pelaz L, Marques L A and Barbolla J 2004 *J. Appl. Phys.* **96** 5947
[4] Muller T, Heinig K-H and Muller W 2002 *Appl. Phys. Lett.* **81** 3049
[5] Kachurin G A, Cherkova S A, Volodin V A, Kesler V G, Gutakovsky A K, Cherkov A G, Bublikov V A and Tetelbaum D I 2000 *Nucl. Instrum. Methods* B **222** 497 and references therein
[6] Chaughari P S, Bhave T M, Kanjilal D and Bhoraskar S V 2003 *J. Appl. Phys.* **93** 3486
[7] Arnoldbik W M, Tomoxeiu N, van Hattum E D, Lof R W, Vredenberg A M and Habraken F H P M 2005 *Phys. Rev.* B **71** 125329
[8] Antonova I V, Gulyaev M, Savir E, Jedrzejewski J and Balberg I 2008 *Phys. Rev.* B **77** 125318
[9] Toulemonde M, Dufour Ch, Meftah A and Paumier E 2000 *Nucl. Instrum. Methods* B **166/167** 903
[10] Meftah A, Brisard F, Constantin J M, Dooryhee E, Hage-Ali M, Hervieu M, Stoquert J P, Studer F and Toulemonde M 1997 *Phys. Rev.* B **49** 12457
[11] Antonova I V, Shaimeev S S and Smagulova S A 2006 *Semiconductors* **40** 557
[12] Antonova I V, Gulyaev M B, Yanovitskaya Z Sh, Valodin V A, Marin D V, Efremov M D, Goldstein Y and Jedrzejewski J 2006 *Semiconductors* **40** 1198
[13] Heinz B, Mertz M, Widmayer P and Ziemann P 2001 *J. Appl. Phys.* **90** 4027
[14] Schoenfeld O, Zhao X, Hempel T, Blaesing J, Aoyagi Y and Sugano T 1994 *J. Cryst. Growth* **142** 268
[15] Balberg I 2005 *Proc. 1st Int. Workshop on Semiconductor Nanocrystals (Hungarian Academy of Science, Budapest, Sept.)* p 291
[16] Volodin V A, Efremov M D, Gritsenko V A and Kocubei S A 1998 *Appl. Phys. Lett.* **73** 1212
[17] Morell G, Katiyar R S, Weisz S Z, Jia H, Shinar J and Balberg I 1995 *J. Appl. Phys.* **78** 5120
Posada I, Balberg I, Fonseca L F, Resto O and Weisz S Z 2001 *Mater. Res. Soc. Symp. Proc.* **638** F14.44
[18] Dovrat M, Oppenheim Y, Jedrzejewski J, Balberg I and Sa'ar A 2004 *Phys. Rev.* B **69** 155311
Dovrat M, Goshen Y, Popov I, Jedrzejewski J, Balberg I and Sa'ar A 2005 *Phys. Status Solidi* c **2** 3440
Sa'ar A, Reichman Y, Dovrat M, Kraf D, Jedrzejewski J and Balberg I 2005 *Nano Lett.* **5** 2443
Sa'ar A, Dovrat M, Jedrzejewski J and Balberg I 2007 *Physica* E **38** 122
[19] Viera G, Huet S and Boufendi L 2001 *J. Appl. Phys.* **90** 4175
[20] Cerofolini G F and Meda L 1987 *Phys. Rev.* B **36** 5131
[21] Adekoya W O, Hage M, Muller J C and Siffert P 1987 *Appl. Phys. Lett.* **50** 1736
[22] Van Dillen T, Polman A, Onck P R and Van der Giessen E 2005 *Phys. Rev.* B **71** 024103
[23] Van Dillen T, de Dood M J A, Penninkhof J J, Polman A, Roorda S and Vredenberg A M 2004 *Appl. Phys. Lett.* **84** 3591
[24] Youngs I J 2003 *J. Phys. D: Appl. Phys.* **35** 3127